THE JOURNAL OF PHYSICAL CHEMISTRY C

Article

pubs.acs.org/JPCC

Conformational Behavior of Genetically-Engineered Dodecapeptides as a Determinant of Binding Affinity for Gold.

Stefano Corni,*[,†] Marketa Hnilova,[‡] Candan Tamerler,[‡,§] and Mehmet Sarikaya*[,‡,§,⊥]

[†]Center S3, CNR-Institute of Nanoscience, via G. Campi 213/A, 41125 Modena, Italy

[‡]Materials Science and Engineering, [§]Chemical Engineering, and [⊥]Oral Health Sciences, Genetically Engineered Materials Science and Engineering Center, University of Washington, 302 Roberts Hall, Seattle, Washington 98195, United States

Supporting Information

ABSTRACT: Genetically engineered solid binding peptides, because of their unique affinity and specificity for solid materials, represent a promising molecular toolbox for nanoscience and nanotechnology. Despite their potential, the physicochemical determinants of their high affinity for surfaces remain, in most cases, poorly understood. Here we present experimental data and classical atomistic molecular dynamics simulations for two gold binding dodecapeptides (AuBP1 and AuBP2, Hnilova, M. et al. *Langmuir* **2008**, *24*, 12440) and a control peptide that does not bind to gold, to unravel the key microscopic differences among them. In particular, by means of extensive sampling *via* replica exchange simulations, we show here that the conformational ensemble of the three peptides in solution and on the gold surface can be examined, and that the role played by their different conformational flexibility can be analyzed. We found, specifically, that AuBP1 and AuBP2 are much more flexible than the control peptide, which allows all the potential Au-binding amino acids present in these AuBPs to concurrently bind to the gold surface. On the contrary, the potential Au-binding amino acids in the rigid control peptide cannot contact the surface all at the same time, hampering the overall binding. The role of conformational flexibility has been also analyzed in terms of the configurational entropy of the free and adsorbed peptides. Such analysis suggests a possible route to improve upon current flexible gold binding peptides.

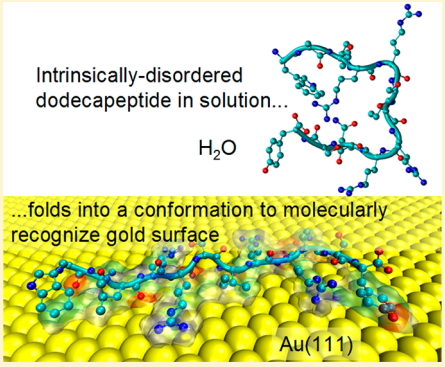

INTRODUCTION

Several natural processes, for example, biological hard-tissue growth,[1] cell-surface adhesion,[2] and inhibiting ice formation inside cells,[3] involve proteins or peptides capable of recognizing solid surfaces.[4−6] Through inspiration from Nature, proteins and peptides that specifically bind to a given inorganic solid surface have been obtained experimentally by combinatorial biology.[5,7−10] The technological potential of such artificially selected polypeptides has been previously recognized,[4,11−13] and they have been used as the key building blocks in the implementation of molecular biomimetics in practical applications.[5] In this context, until now, more than 20 different sets of peptides have been biocombinatorially identified that are capable of recognizing surfaces of a variety of metals, oxides, and semiconductors.[10] These peptides, their conjugates, and variations have been used in the synthesis of inorganic nanoparticles,[14] immobilizing nanoentities on solid surfaces,[15−17] and biofunctionalization of solids for a variety of nanotechnological[18] and biotechnology applications.[19]

Recently, two new dodecapeptides have been selected for gold binding.[20] These are AuBP1 and AuBP2, with sequences WAGAKRLVLRRE and WALRRSIRRQSY, respectively. (One-letter codes for amino acids mentioned in the text: W: tryptophan; A: tlanine; G: glycine; K: lysine; R: arginine; L: leucine; V: valine; E: glutamic acid; S: serine; I: isoleucine; Q: glutamine; P: proline; Y: tyrosine; M: methionine.) Molecular adsorption studies carried out by surface plasmon resonance (SPR) spectroscopy measurements indeed confirmed the high affinity of AuBP1 and AuBP2 for gold in the submicromolar range, and the most stable structure of each of these peptides in solution was determined by computational methods.[20] While it was apparent from gold affinity measurements on the cyclized forms of AuBP1 and AuBP2 that molecular architectures play an important role, the exact molecular conformations of the peptides on the gold surface remain unknown. The specificity of small peptides such as AuBP1 and AuBP2 (12 amino acid long) recognizing solid surfaces specifically is intriguing as these peptides in solution often are quite flexible, that is, intrinsically disordered, and thus may have multiple conformations in the absence of a substrate. Therefore, there are fundamental questions whether peptides change conformations on the surface and how the specific sequences affect their stability on the crystallographically flat gold surface. Specifically, here we use atomistic classical Molecular Dynamics (MD) enhanced by an accelerated conformational sampling technique (replica-exchange molecular dynamics REMD)[21] to characterize the conformations of AuBP1 and AuBP2 in solution and to investigate if these conformations change upon binding to the

Received: April 24, 2013
Revised: July 10, 2013
Published: July 17, 2013

Au(111) surface. Moreover, we discuss how these conformational characteristics of the peptides relate to the experimentally determined binding affinity for the gold surface.

Classical MD has been chosen here since at present it is the best compromise between accuracy and computational feasibility for studying peptide adsorption on solid surfaces.[22,23] Quantum mechanical calculations have been mostly limited to the study of single amino acids on gold (minimum energy structures and neglecting solvent effects).[24−28] Only recently, *ab initio* molecular dynamics (AIMD) simulations have been used to study a solvated minimal protein (a polyserine β-sheet in water) on a Au(111) surface.[29] Although this work delivered relevant information on the studied system (showing its capability to discriminate between the Au(111) surface sites and highlighting the role of hydration water), the accessible AIMD time and length scales are still rather limited and cannot be used to study conformational changes of dodecapeptides.

The adsorption of AuBP1 and AuBP2 on Au(111) has not been previously investigated even with classical MD. However, previous studies have addressed the interaction of other proteins and peptides with the gold surfaces at the classical MD level.[30−38] Some of these studies focused specifically on gold-binding peptides (GBPs). Braun et al.[30] studied a 3-repeat GBP (42 amino acid long)[39−41] on the Au(111) and Au(211) surfaces in water, finding different interaction energies and water content for the peptide-surface interfaces. Heinz et al.[33,34] studied other peptides on Au(111), Au(100), Pt(111), and mixed Au/Pt surfaces with a force field tuned to reproduce the hydrophilicity of the Au surfaces.[35] The concept of soft-epitaxy was introduced[33] and used to explain the binding capabilities of different peptides on different crystal faces. Vila Verde et al.[36] compared a multiple-repeat GBP[39] and a non-GBP on Au(001) by using a force field also tuned on gold hydrophilicity. This study suggests that the higher flexibility of the GBP with respect to the non-GBP made easier the conformation rearrangements needed to increase the direct peptide-surface contact; this is similar to the findings that we are presenting here for AuBP1 and AuBP2. Later on, the study was extended to various homopeptides and the relation between flexibility and binding was confirmed.[37] The role of flexibility was also commented on by Yu et al.[38] MD have been also used to study the interaction of genetically engineered peptides interacting with inorganic surfaces other than gold, including rutile,[45] quartz,[46] hydroxyapatite,[47] silicon,[48] graphite, and carbon nanotubes.[49,50]

The basis of the interaction between the peptides and gold is related to the high-affinity of some chemical groups within the peptide residues for gold. The presence of such residues does not guarantee high affinity of the whole peptides for gold, as we demonstrate in the present work. Yet, in the analyses that follow, we shall frequently make reference to the different propensity of individual amino acids with affinity to bind to gold. Therefore, it is worthwhile to introduce such propensities here. There is no established experimental gold-affinity scale for single amino acids. Nevertheless, the *corpus* of works on small peptides and mutated proteins leads to some consensus that there are amino acids with high propensity to bind to gold (in the following, we call these "potential Au-binding amino acids"). We summarize in Table 1 the potential Au-binding amino acids as found from the experimental literature.

With the exception of Willet et al.[51] there is consensus in the experimental data that His, Trp, Cys, and, to a lower degree, Met are potential Au-binding amino acids. We interpret the constant presence of these amino acids in the lists in Table 1 as a sign of their strong affinity for Au. It is well-known that Cys binds to gold strongly *via* S−Au covalent bond, and we shall not consider it further since our work is concerned with Cys-free gold binding peptides. Tyr is also present, although not in the first positions, in three experimental works out of five. Arg is also found in three works, although in one of them (Hnilova et al. 2008)[20] Arg is overrepresented both in strong-binding AuBPs and in weakly gold binding peptides, which makes the role of Arg unclear. Finally, Lys is also identified in two studies. Thr, Gln, and Ile appear only in one study each, and are likely related to specific aspects of the corresponding experimental systems rather than to a genuine high affinity for Au. Taking into account all these considerations, we propose to summarize the current status of experimental knowledge on potential Au binding amino acids with the following scale (Cys not considered): His ≈ Trp > Met > (Tyr, Lys, Arg) where the relative order within the last group is unclear.

Table 1. Summary of the Potential Gold Binding Amino Acids (AAs) Obtained in Various Experimental Studies[a]

ref	system	potential Au binding AAs
Willet et al. 2005[51]	homo-octa/decapeptides	Thr, Arg
Peelle et al. 2005[52]	homohexapeptides exposed on cells	His, Met, Trp, Cys
Peelle et al. 2005[52]	up-modulation of binding in XHXHXHX peptides	His, Trp, Lys, Met, Cys, Arg, Gln, Tyr
Hnilova et al. 2008[20]	AA enrichment/depletion in dodeca-AuBPs	Trp, Cys, His, Tyr, (Arg),[b] Ile, Met
Cohavi et al. 2010[53]	homotripeptides fused to a protein	His, Trp, Lys, Met, Tyr[c]

[a]The amino acids are given in decreasing gold-binding propensity order (i.e., the first has the highest propensity to bind gold among all the considered amino acids). "System" refers to the kind of molecules used in the experiments. Potential Au-binding AAs have been identified for each work as those that provide a binding higher than the average between the best and the worst reported binders. For the XHXHXHX peptides we report the AAs that clearly up-modulate binding vs Ala.[52] [b]Arg is found to be overrepresented both in AuBPs and in peptides having a weak binding to gold, so its role remains unclear. [c]Cys and Pro were not considered.

From the computational point of view, adsorption energies of amino acids have been calculated by using CVFF-METAL[42] and CHARMM-METAL[43] force fields. Arg, Trp, Gln, Met, Tyr and Asn are the amino acids with more exothermic adsorption on Au, using the most recent CHARMM-METAL.[43] An adsorption free-energy scale for all the amino acids on Au(111) in water has been provided by Hoefling et al.[44] based on the same force field used in the present work,[54] showing that the intrinsic affinity of the natural amino acids toward gold is dependent on the chemical nature of their side chains. In this affinity scale, the amino acids that have a higher than the average affinity for Au(111) are Tyr, Phe, His, Trp, Met, Arg; Lys is on the average. The first five of these (Tyr to Met) have basically the same adsorption energy within the statistical errors. This list qualitatively matches the experimental findings above, including the borderline role of Arg and Lys, except for the presence of Phe among the potential Au-binding amino acid. Since Phe is not present in the peptides considered here, this is immaterial. We also recall that these are the results for the amino acids at the water/gold interface. In *vacuo*, other chemical groups present in peptides (such as hydroxyl and carboxilate groups) were found to bind to gold.[27]

dx.doi.org/10.1021/jp404057h | J. Phys. Chem. C 2013, 117, 16990−17003

To highlight the peculiarities of AuBP1 and AuBP2 we have also investigated a control (nongold binding) peptide, whose sequence is PPPWLPYMPPWS, a quartz-binding peptide, that is, QBP1. This peptide was originally *de novo* designed *via* a combined biocombinatorial and bioinformatics approach to bind to quartz surfaces;[55] here we also report the experimental characterization of its binding to gold *via* SPR spectroscopy. The binding affinity of this peptide for gold was also computationally predicted to be smaller than those of either AuBP1 or AuBP2, conforming the experimental results. The choice of QBP1 as a control peptide is motivated by various reasons: It contains a significant number of potential Au-binding amino acids (2 Trp's, Met, Tyr) and still it is not a gold binder; It is an inorganic binding peptide itself, so it has no intrinsic feature that prevents its binding to surfaces; Its sequence has been obtained on a similar ground as those of the AuBPs, that is, by biocombinatorial methods. The main features of the three peptides studied in this work are summarized in Table 2.

Table 2. Main Characteristics of the Three Peptides Studied in This Work. pI Is the Isoelectric pH and MW is the Molecular Weight

Name	*Sequence**	*pI#*	*MW#*	*Hydropathicity#*
AuBP1	WAGAKRLVLRRE	11.71	1454.7	-0.567
AuBP2	WALRRSIRRQSY	12.00	1591.8	-1.267
QBP1	PPPWLPYMPPWS	5.95	1467.7	-0.650

*Notation: gray = hydrophobic, orange = aromatic, blue = basic, red = acidic, and green = hydrophilic uncharged. #Computed using ProtParam computational tool (expasy.org).

An important property of the studied peptides is their amino acid sequence, which includes both the type of residues (i.e., the amino acid composition of the peptide) and their sequential order. All the physicochemical properties of the peptides, including those extensively analyzed in this paper such as the conformational flexibility, are encoded in the sequence. On the basis of the amino acid composition alone (i.e., discarding all the complex cooperative effects that take place among the amino acids of a peptide and that are also sensitive to the amino acid ordering), it is difficult to justify why the control peptide QBP1 is a much worse Au binder than the two AuBPs. In particular, if we compare the amino acids content of QBP1 with that of AuBP1 in terms of potential Au-binding amino acids, we find that the former contains 2 Trp, 1 Met, 1 Tyr, no Arg, and no Lys, while the latter contains 1 Trp, no Met, no Tyr, 3 Arg, and 1 Lys. In other words, QBP1 contains a larger number of strong Au-binding amino acids (Trp, Met) than AuBP1. The latter can compensate the gap only partially because of a larger number of borderline Au-binding amino acids (e.g., Arg, Lys). Therefore, there should be physicochemical properties of the peptide, codified by its sequence *via* specific folding patterns which in turn allow AuBP1 to better exploit its Au-binding potential than QBP1. The dodecapeptide QBP1 is rich in Pro residues, which are absent in AuBP1 and AuBP2, that typically confer a greater rigidity to the protein structure. Therefore, one can anticipate that different conformational flexibility of the peptides encoded in their sequences, and hence the different physical conformations accessible to them, plays a key role in overruling the trend imparted by the chemical amino acid content alone.

The computational results presented here reveal a microscopic picture of the molecular mechanisms of peptide binding to gold surfaces, and confirm the experimental finding that AuBP2 and AuBP1 bind gold stronger than the control peptide QBP1. In particular, calculations show that all the peptides change their conformations upon binding with respect to those in solution, but QBP1, the most rigid, is unable to achieve a conformation where the attractive interactions with gold would be maximized. On the contrary, AuBP1 and AuBP2 are conformationally flexible, and readily adapt to the atomically flat gold surface. The consequences of such flexibility (large configurational entropy losses upon adsorption) are also quantified and discussed, leading to the suggestion that peptides with even higher gold affinity than AuBP1 and AuBP2 may be rationally designed based on the key guidelines resulting in this work.

METHODS

Surface Plasmon Resonance (SPR) Binding Experiments. SPR measurements were performed using a four channel instrument (Kretschmann configuration) developed by the Radio Engineering Institute, Czech Republic. It was equipped with a polychromatic light source (Ocean Optics LS1). The instrument can detect changes at a level of 0.0001 refractive index unit, and is temperature controlled. Buffer and peptides solutions were degassed to avoid bubbles in the flow cell. First, a phosphate buffer solution (1:3 mix of 10 mM KH_2PO_4, 10 mM K_2HPO_4, and 100 mM KCl) was allowed to flow over the surface until a stable baseline signal was established. Then, peptide solutions in phosphate buffer at 0.46 μM (AuBP1, AuBP2, QBP1) and 5 μM (QBP1) concentrations were allowed to flow over the Au surface and peptide adsorption kinetics were monitored. After the surface coverage reached or neared equilibrium, the phosphate buffer solution was allowed to flow again, and desorption of the peptide was monitored. The system was then cleaned using a 1% SDS + 0.1 M NaOH solution, followed by a 0.1 M HCl solution, and finally DI water. For data analysis purposes, the SPR signal was calibrated in order to calculate adsorbed mass per cm^2 from the surface plasmon wavelength shift given by the raw data.

Simulations. Peptides have been described by using the OPLS/AA force field, whose quality in describing peptide folding is reasonable.[56] Explicit SPC water was used in this study. The SPC water model (that is similar to the TIP3P model) is compatible with OPLS[57] and has been already used together with OPLS-AA to describe folding in solution.[58] For the simulations with the Au(111) surface, we exploited the GolP force field.[54] Within this force field, the gold surface is polarizable, and can locally develop net charges, although it remains overall neutral. Preliminary tests have shown that this force field can reproduce experimental energy results for small molecules in controlled conditions[54] and provide a gold wetting coefficient greater than or equal to 1[59] in line with experimental findings.[60] Extensive free-energy classical MD simulations on the adsorption on Au of single amino acids have shown a trend coherent with experimental data.[44] GolP has been recently extended to another protein force field (CHARMM) and to another Au surface, Au(100).[61]

All the simulations were performed in the canonical (i.e., NVT) ensemble. For the peptides in solution, the volume V was obtained by preliminary NPT simulation at 300 K; for the peptide on the surface V has been adjusted so to yield SPC bulk

dx.doi.org/10.1021/jp404057h | J. Phys. Chem. C 2013, 117, 16990−17003

water density in the water layer far from the surface and from the peptide. Particle-Mesh Ewald method has been used for electrostatic. The cutoff for Lennard-Jones interactions was 1.1 nm.

Probing conformational space of even a 12-amino acid peptide is still a daunting task for atomistic simulations in explicit water. We have performed long replica exchange molecular dynamics (REMD) simulations.[21] REMD consists in running several classical MD simulations in parallel, each one at a different temperature. At constant time intervals, the potential energy of the instantaneous conformation from the different simulations is compared, and the temperatures of the compared simulations are swapped or not following a Monte Carlo rule. Therefore, each conformation experiences a random-walk along the temperature dimension. This allows exploration of the high temperature regions where the systems can overcome barriers separating conformational basins, and speeds up conformational changes also accelerating diffusion in the conformational space. REMD simulations also yield the correct statistical sampling at each temperature. On the other hand, they are computationally time consuming because of the need to simulate several replicas of the system in parallel, requiring either supercomputers or distributed computing to be performed. Moreover, it is imperative to mention that time in REMD does not have a direct physical meaning, since the dynamics is accelerated by the exchanges of replicas.

REMD has been already used to simulate QBP1 in ref 46 with a different force field (CHARMM and TIP3P) and with replicas in the interval 290 K to 400 K; similar configurations were found as those obtained here.

In our simulations, we used 156 replicas for the simulations without surface and 121 for the simulations with the surface. The temperature of the replicas ranged from 300 to 1000 K, and was selected with the procedure described in ref 62. The average time between exchanges of replicas was around 3 ps for the simulations without surface, and 1.5 ps for the simulations with the surface. Acceptance ratios for replica exchange and diffusion of replicas in the temperature space are shown in Supporting Information, Figure S3. Simulations started with the peptides in the fully extended conformation as obtained by the Tinker program *protein*.[63] REMD simulations were run until the population of the main conformation (averaged over running windows 1.5 ns long) did not show net drifts, and ranged from 9 to 24 ns per replica depending on the peptide. The aggregated simulation time was, therefore, around 1−2.5 μs per peptide. The clustering algorithm by Daura et al.,[64] with a threshold of 0.3 nm on the backbone RMSD to identify structures belonging to the same cluster, was used to define distinct conformations *via* the GROMACS g_cluster utility. All the simulations have been performed with the GROMACS 4.0 code[65] on a IBM SP6 supercomputer.

The possible shortcomings of REMD to study peptides on surfaces have been investigated in depth by Latour and coworkers.[22,66] In particular, they discuss the incapability of REMD to provide free-energy of adsorption from relative populations since the ratio adsorbed versus desorbed is too small at room temperature. To this end, they introduced a biased-REMD that couples REMD with umbrella sampling to yield adsorption free energy profiles. Moreover, they have developed methods that are less computational intensive than REMD while still efficiently exploring the conformational space (TIGER and TIGER2).[67] More recently, non-Markovian metadynamics[68] coupled to Solute Tempering[69] has been used to study a titania binding peptide,[70] and nonequilibrium thermodynamics integration has been used to calculate binding free-energy for the met-enkephalin pentapetide on graphite.[71] In this paper, we are not presenting adsorption free-energy data and, therefore, a biased-REMD approach or metadynamics is not mandatory. Moreover, TIGER and TIGER2 are not implemented yet in standard simulation packages such as GROMACS. For these reasons, we decided to rely on the standard REMD approach.

To address the problem of the kinetic trapping of peptides in a given configuration due to the interaction with the surface, we used very high temperatures (up to 1000 K as mentioned above) in the REMD, and we checked that at these temperatures the peptide can detach almost completely from the surface. Of course this choice comes with a computational cost, not only because more replicas must be used to reach such a high T, but also because simulations should be run for a longer time so to allow the system to diffuse on the larger temperature interval.

Solvent Accessible Surface Area (SASA) was also used to characterize the peptides. Here SASA was calculated using the algorithm proposed in ref 72 as implemented in the VMD code.[73]

RESULTS AND DISCUSSION

3.1. SPR Affinity Measurements for AuBP1, AuBP2 and QBP1 on Gold. In various experimental studies, chemically synthesized AuBPs and QBP1 peptides were reported to exhibit excellent binding affinities to their respective materials, that is, gold and silica, with adsorption parameters roughly corresponding to frequently studied molecules that form self-assembled monolayers (SAMs).[13,20,55,74−76] Here, we test the binding characteristics of AuBP1, AuBP2, and QBP1 peptides with respect to gold using a previously established SPR technique.[20,76] The peptide adsorption behavior was carried out in water-based solvents under neutral pH. Initially, we monitored the adsorption kinetics of 0.46 μM AuBP1, AuBP2, and QBP1 peptide solutions onto the flat Au surface. The peptide QBP1, at the same concentration, did not bind onto the solid gold surface detectibly; subsequently, therefore, we determined the adsorption binding kinetics of a 5 μM QBP1 peptide solution (~10-fold increase). Raw kinetic data of AuBP1, AuBP2 (0.46 μM), and QBP1 (5 μM) on Au surfaces from SPR tests were fitted with a modified Langmuir adsorption model[77] as shown in Supporting Information Figure S1. The values of SPR shifts and the corresponding adsorbed peptide mass per cm^2 after the washing step are plotted in Figure 1.

As evidenced in Figure 1, the peptides exhibited significant solid recognition, that is, both AuBP1 and AuBP2 adsorbed onto the gold surface with high affinity, whereas the QBP1 adsorbed mass on the gold substrate was undetectably small when the same peptide concentration as those of the AuBPs was used. When the QBP1 concentration was increased ~10 times, still only a small amount of adsorbed peptide was detected, equivalent to a fraction of the adsorbed masses of AuBPs. It should be pointed out here that while both gold-binding sequences displayed strong binding to the gold surface, at the same tested concentration we recorded a difference in adhered masses for AuBP1 and AuBP2. Specifically, the estimated surface-adsorbed masses of 39.5 ± 2.6 ng/cm^2 and 17.4 ± 0.8 ng/cm^2 for AuBP2 and AuBP1 peptides,

dx.doi.org/10.1021/jp404057h | J. Phys. Chem. C 2013, 117, 16990−17003

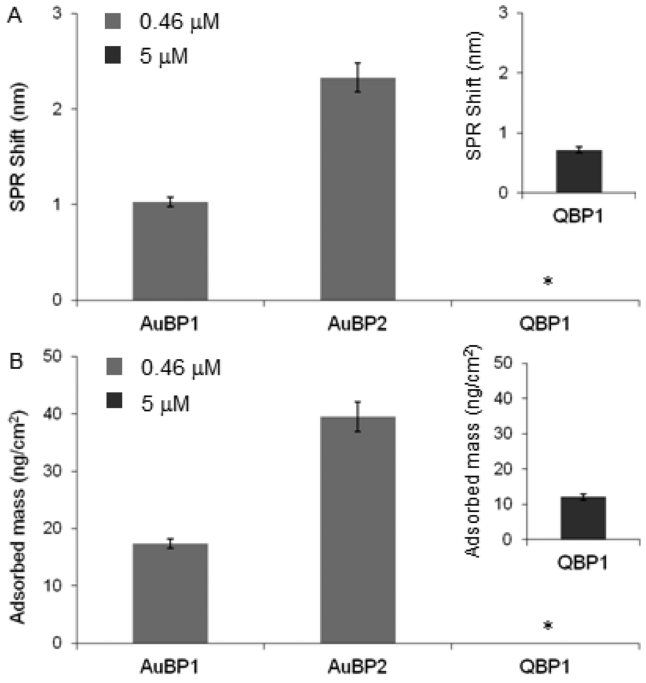

Figure 1. Binding affinity of synthetic AuBP1, AuBP2, and QBP1 *via* SPR. (A) Recorded SPR shifts for 0.46 μM peptide concentrations on gold (insert shows recorded SPR shift for 5 μM QBP1). (B) Quantification of adhered peptide mass/cm^2 calculated from recorded SPR shifts presented in panel A. Insert shows calculated adsorbed peptide mass/cm^2 for 5 μM QBP1. (*) No SPR shift was observed for 0.46 μM QBP1.

respectively, suggest marginally better binding affinity for AuBP2 compared to that for the AuBP1 sequence.

3.2. Peptide Conformations in Water by REMD Simulations. *QBP1.* The REMD simulation, started by the fully extended conformation, rapidly converges to a dominant cluster (relative population, ~90%), as shown by Figure 2. Only a small fraction of the initial, extended, conformation survives at the end of the REMD.

The representative structures of each configurational cluster are represented in Figure 2. The cluster that dominates the population presents a turn involving the central residues 5−7; this confers a hairpin-like geometry to the peptide. To explore the average configurational properties, we calculated a 3D Ramachandran plot obtained for the last 3 ns of the dynamics which is reported in Figure 3 (this contains contributions from all the conformations).

As expected on the basis of the high proline contents of QBP1 (i.e., 50% of the amino acids in the QBP1 sequence are proline), the resulting structure of the peptide has a strong peak at the Φ/Ψ values proper for polyproline II conformation. To further check the content of polyproline II conformation in the dominant cluster, we calculated the chirality index G[78] for QBP1, averaging over the entire population of the dominant cluster. As expected, the results also confirm that the portions Pro_1-Pro_3 and Pro_9-Trp_{11} have PPII-like conformations. The same conformation had also been obtained for QBP1 with a different force field (CHARMM) in a recent work by Oren et al.[46] From these studies, it becomes clear that there is a convergence of the values from different force fields to the same structure, confirming the reliability of these results.

AuBP1. Contrary to the case of QBP1, the dominant cluster of AuBP1 represents only 50% of the population of conformations, and which fluctuates on the REMD time scale (Figure 4).

Interestingly, the conformation of the main cluster is the same proposed by Hnilova et al.[20] In this reference, a different computational approach (based on implicit solvent models with refinement in explicit solvent) was used to predict the most stable structure. The agreement between the two methods supports the reliability of the results.

Finally, to synthetically characterize the AuBP1 structure, we calculated the average SASA also for AuBP1, finding a value of 1601 ± 12 Å^2. This value is larger than for QBP1, due to the more extended conformation, and it is also representative of a larger hydrophilicity of AuBP1 than QBP1 (as expected from the sequences).

AuBP2. Clustering results for AuBP2 exhibit an even larger variety of conformations than that for AuBP1. Evolution of the populations of the four most represented clusters is reported in Figure 5. It should be noted that, in the case of AuBP2, the initial conformation of REMD was not the extended structure, as observed for AuBP1 and QBP1, but resulted from a preliminary multiple simulated annealing procedure. In fact, on the basis of the AuBP1 REMD simulation, it was clear that convergence to equilibrium population starting from extended simulation requires tens of nanoseconds, which correspond to a considerable computational effort. A preliminary simulated annealing allows shortening the transition regime in the REMD simulation and, thus, the overall computational time. Moreover, it does not compromise comparability with the other peptides since the REMD are long enough to lose memory of the initial state preparation.

The population of the main cluster at the end of the dynamics is around 35−40%, which is sensibly lower than for AuBP1, indicating a more flexible structure able to probe a larger conformational space at room temperature. To exemplify such structures, we report in Figure 5 the representative structure for each of the four most populated clusters. A comparison of the representative structures for AuBP2 with those for AuBP1 shows that AuBP2 appears to have more open conformations than AuBP1. This is also affirmed by the average value of SASA being 1782 ± 17 Å^2 for AuBP2, around 10% larger than that of AuBP1. Interestingly, an open structure was also found in ref 12 that was very similar to the Cluster 2 found here.

It is significant to emphasize that for flexible peptides such as AuBP1 and AuBP2, it is difficult to define a single peptide conformation. Rather, the concept of ensemble of conformations[48] should be used: each peptide is exploring multiple conformations, each with its own probability. For AuBP1, this ensemble of conformation is dominated by the closed structure shown in Figure 4, but it also assumes the other conformations, depicted in the figure, as well. For AuBP2, the ensemble of conformations has basically no dominant structure, since the most populated clusters have very similar populations. It is imperative to comment that conformations are defined here only in terms of the backbone atoms of the peptides (i.e., the peptide N,C, and the Cα). Side chains are extremely flexible, and add several other degrees of freedom to the conformational space.

3.3. Conformational Rearrangements on Gold. To verify how the adsorption on the gold surface can modify the conformation of the three peptides under study here, we performed REMD simulations of these peptides on gold in water. The initial peptide structures of these REMDs were

dx.doi.org/10.1021/jp404057h | J. Phys. Chem. C 2013, 117, 16990−17003

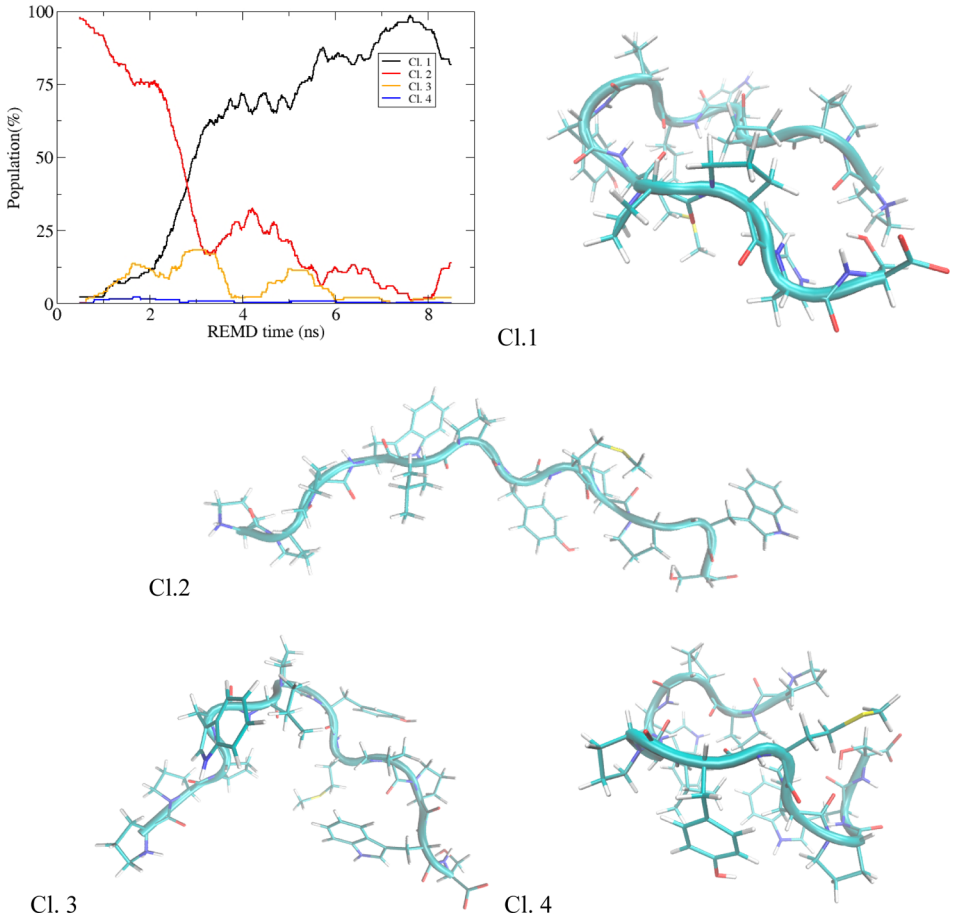

Figure 2. Relative populations of the four most populated clusters for QBP1 in water as a function of the simulation time, and representative structure for each cluster.

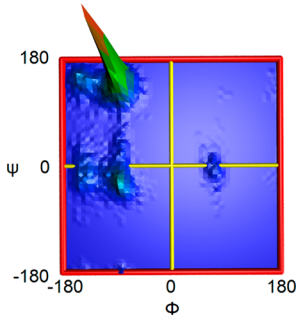

Figure 3. 3D Ramachandran plot for the last 3 ns of REMD for QBP1. The high peak corresponds to Φ/Ψ angles typical of a polyproline II conformation.

those representatives of the most populated conformational clusters resulting from the REMD in water, that is, the conformations reported in Figures 2, 4, and 5 for QBP1, AuBP1, and AuBP2, respectively. Although these are quite different, they all rapidly converge to very similar conformations on gold. In fact, after roughly 10 ns of REMD, all the peptides have practically a single conformation of the backbone that dominates the conformational ensemble (see Supporting Information, Figure S2), while the precise arrangement of the side chains is quite different in each case. The representative dominant conformations are shown in Figure 6 for all the peptides studied in this work.

For AuBP1 and AuBP2, these conformations are close to the fully extended ones. This represents a large deformation with respect to the predominant structures of AuBP1 and AuBP2, which are almost cyclic. The conformational richness of AuBP1 and AuBP2 in solution, on the other hand, shows that these peptides are highly flexible and can easily modify their structure. The peptide moieties lay parallel to the gold, and the backbone is in contact with the surface. The dominant structure for QBP1 (accounting for ∼80% of the conformational ensemble) is also more extended than in solution, but it is not fully extended, as found for the gold-binding peptides. The QBP1 structure on gold is related to the dominant QBP1 structure in solution: the former can be obtained from the latter by opening the hairpin folding. Moreover, the QBP1 structure on gold resembles a weakly populated structure (Cl.3 in Figure 2) obtained for QBP1 in solution. From the REMD studies carried out on the surface, a more extended conformation is also found, which accounts for ∼5% of the conformational ensemble. Among all the observed structures for QBP1, only part of the backbone is in direct contact with the surface, which is attributed to the geometric constraints induced by the presence of proline residues.

The orientational preferences of complex adsorbates on a surface are important in determining the creation of ordered structure on the surface (notwithstanding the order that can arise from coadsorbate interactions, which is outside the scope of the present article). Therefore, we have investigated whether there are preferential orientations of the peptide backbone with

dx.doi.org/10.1021/jp404057h | J. Phys. Chem. C 2013, 117, 16990−17003

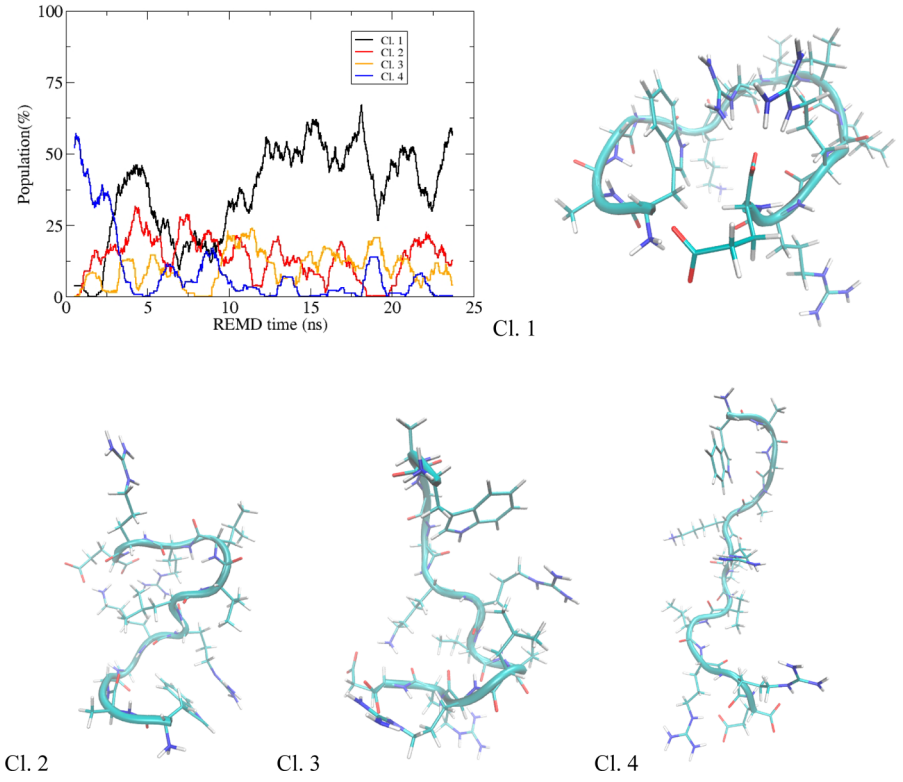

Figure 4. Relative populations of the four most populated clusters for AuBP1 in water as a function of the simulation time, and representative structure for each cluster.

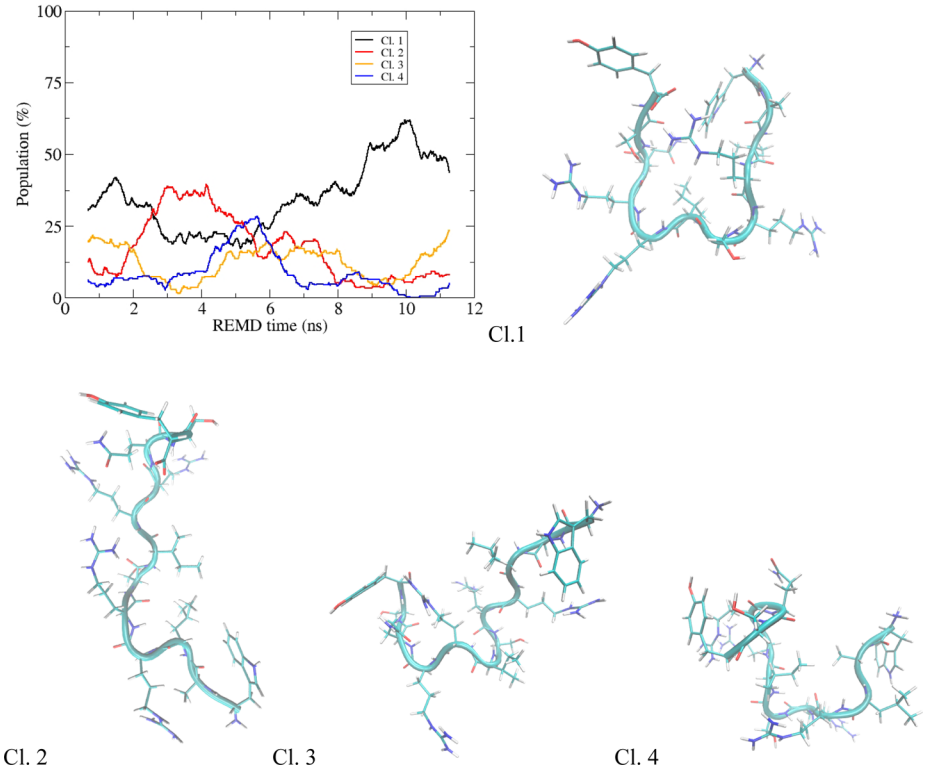

Figure 5. Relative populations of the four most populated clusters for AuBP2 in water as a function of the simulation time, and representative structure for each cluster.

respect to the gold lattice for the three peptides. To this aim, for each peptide we defined a vector along a linear portion of the backbone which was chosen to be unaffected by conformational changes. (The vector connects two Cα in the peptide backbone; we have considered the residues 2 and 6 for QBP1, 3, and 11 for AuBP1, 6, and 9 for AuBP2.) The angle

dx.doi.org/10.1021/jp404057h | J. Phys. Chem. C 2013, 117, 16990−17003

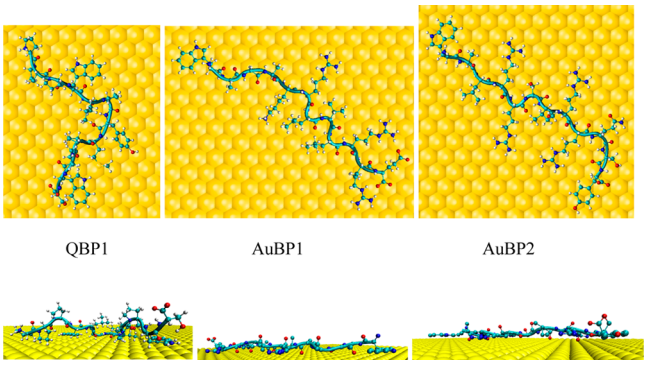

Figure 6. Representative structures of the dominant conformational clusters remaining in the last 1.5 ns of the REMD on Au(111) surface for the three peptides studied herein. Upper panels: top views. Lower panels: side views. The depicted orientation of the peptides with respect to the gold lattice are probable, but not necessarily unique, orientations (see Figure 7).

between this vector and the [112] direction (the horizontal direction in Figure 6) is calculated for all the snapshot in the last 3 ns of the REMD trajectory, and the results are binned in histograms. They are reported in Figure 7.

The unreconstructed (111) surface has a 3-fold symmetry; therefore, orientation angles can always be mapped in the interval [0°,120°], and, if the interactions from the second and further gold layers are neglected, the symmetry on the surface layer can be assumed as 6-fold, so, the angles can be mapped to [0°,60°]. Although this assumption is an approximation, it allows doubling the number of sampled point per angle bin, reducing statistical noise. In fact, even if REMD is accelerating the sampling of the conformational space, 3 ns is not enough to recover the correct 3-fold periodicity in the angle. We sacrificed characterizing the (small) differences due to the second or more gold layers for a better sampling, and, therefore, in Figure 7 the angles are mapped in the interval [0°,60°].

The most striking difference in Figure 7 is that of QBP1 vs the two gold binding peptides, AuBP1 and AuBP2. As it became clear, QBP1 has no preferred orientation (signaled by an essentially constant probability per angle in the figure), while both AuBP1 and AuBP2 have clear peaks in the probability distribution that signal the existence of preferred orientations. This may be a consequence of the weaker QBP1−gold interactions discussed in the next paragraph. AuBP1, in particular, has a quite sharp and high peak at 40°, which corresponds to the orientation shown in the inset. The existence of preferential orientations is an important finding because it shows that these intrinsically disordered AuBP peptides are able to molecularly recognize the Au(111) surface. Interestingly, the way peptide−solid molecular interaction takes place is reminiscent of the peptide−protein molecular recognition in biology, where the disordered peptides fold upon binding to the protein at specific, high affinity, locations.[79] It should be noted however that even if AuBP1 and AuBP2 display such orientational preferences, these are not very strong (we recall that a probability ratio of 10 corresponds to a free energy difference of ∼6 kJ/mol that can be overcome even by a single H-bond between coadsorbed peptide).

3.4. Comparing the Interaction Strength of QBP1, AuBP1, and AuBP2 with Au(111). The evaluation of the interaction free energy of the peptides with Au(111) would, in principle, be possible by taking the ratio of the population of adsorbed peptides and those in solution resulting from REMD. It is well-known that for free-energy differences between two states larger than a few kcal/mol, reliable statistics cannot be obtained by REMD alone. Even the calculation of adsorption energies is highly demanding (adsorption energy is defined as the difference in the average energy of the entire peptide+gold +water system between the two states: peptide adsorbed on the surface and that in-solution). In fact, this energy value consists of the difference of two large numbers each with a statistical uncertainty to give a relatively small number. Methods to minimize such uncertainty have been proposed.[80,81] Unfortunately, such methods cannot reliably be applied in the present case. (To emphasize this issue, we note that due to the long-range nature of Coulomb interactions, the energy of the system includes a Coulomb contribution for the interaction among the original system and its periodic images that depends on the volume and the shape of the simulation box. In fact, we used different simulation boxes for the peptide on gold and in water alone to minimize the REMD computational costs. In each case, we realize that the contribution from Coulomb interaction among periodic images will not be the same for the two REMD simulations, and will not cancel out when taking the total energy difference to calculate adsorption energies. Therefore,

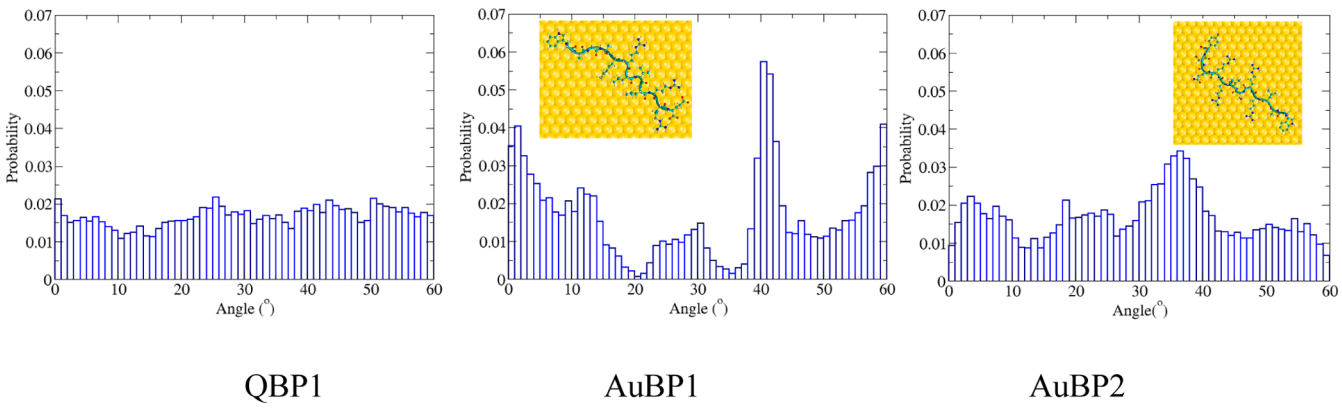

Figure 7. Probability of backbone orientations of peptides on Au(111) during the last 3 ns of the REMD dynamics. The angle is defined with respect to the horizontal direction in Figure 6, those larger than 60° have been remapped to the (approximate) minimal symmetry interval [0°,60°]. Each bar spans an angle interval of 1°, and the height is the probability of the peptide to have an orientation within this interval. In the insets, recurrent orientations for AuBP1 and AuBP2 are illustrated.

dx.doi.org/10.1021/jp404057h | J. Phys. Chem. C 2013, 117, 16990−17003

such adsorption energy would include a spurious contribution of nonphysical origin.)

Considering all the facts described above, we carried out qualitative analysis of the interaction strength based on two indicators of such strength: (i) The number of peptide atoms in contact with the Au surface and (ii) The Lennard-Jones (LJ) interaction energy between the peptide and the gold surface averaged in the last 1.5 ns of REMD. Following ref 54, such Lennard-Jones term effectively includes all the nonelectrostatic peptide-surface interactions (dispersion and repulsion, weak chemisorption effects). It is essential to note that this quantity is only a contribution of the adsorption energy (other contributions being the changes in electrostatics, water−gold LJ, internal energy of liquid water and of the peptide) and it is not directly comparable with the values of enthalpies obtained from experimental adsorption studies.

The average number of contact atoms for each peptide is reported in Table 3. The atoms have been defined to be in contact with the gold surface when their distance to the outer gold atom layer was less than 3.6 Å. The choice of the precise value of this threshold is somewhat arbitrary, but tests performed with other values provided the same picture. The value of 3.6 Å was chosen on the basis of the position of the minimum of the binding free-energy profiles for amino acids on gold, as calculated in ref 44a.

Table 3. Interaction Strength between the Peptides and the Gold Surface[a]

	QBP1	AuBP1	AuBP2
avg no. atom contact	34.62 ± 0.32	43.96 ± 0.23	52.89 ± 0.25
% contact atoms	32.97 ± 0.30%	42.68 ± 0.22%	46.81 ± 0.22%
E_{LJ}^{int} Au−Pept (kJ/mol)	−407.6 ± 6.2	−519.7 ± 4.6	−569.9 ± 6.4

[a]Interaction strength was quantified by the average number of atomic contacts of the peptide with the surface ("avg no. atom contact"), the relative % of peptide atoms in contact with the surface ("% contact atoms") and the Lennard-Jones interaction energy between the peptide and the gold surface, averaged over the last 1.5 ns of the simulation of adsorbed peptide on Au.

The trend from the table is clear whether referring to the absolute contact atom number or to the percentage of peptide atoms in contact with the surface. Both AuBP1 and AuBP2 have a larger number of contacts, that is, a stronger interaction, with gold than QBP1; these are in line with experimental findings. Also, AuBP2 has more contacts to gold than AuBP1, again in line with the experimentally found differences in affinities of these peptides. The trends are confirmed by the LJ interaction energy E_{LJ}^{int}, which shows that AuBP1 and AuBP2 have more favorable interaction with the surface than QBP1, the difference being much larger than the statistical errors of the results. As a technical note, we also calculated the LJ interaction energy E_{LJ}^{int} averaged over the last 3 ns of REMD: the results are all within the error bars reported in Table 3 (the values there are averaged over the last 1.5 ns).

3.5. The Potential Gold-Binding Capabilities of QBP1, AuBP1, and AuBP2, and the Reasons for Different Gold Binding Affinities of the Peptides. As was discussed in the Introduction, it is impossible to justify why QBP1 does not bind to gold while AuBP1 does based solely on the amino acid composition. Since the computational results presented in the previous section also indicate a smaller interaction of QBP1 with the gold surface, it may be valid to analyze the role of amino acid composition of the peptide computationally. Hoefling et al.[44] presented adsorption free energies for all the natural amino acids within the same computational framework that we are using herein. To quantify the gold-binding potential encoded solely in the amino acid composition, that is, by deliberately neglecting all the geometrical constraints, mutual interactions, flexibility changes, etc. that are encoded by the ordered peptide sequence, we can sum up the Hoefling et al. adsorption free-energy of each individual amino acid. The resulting quantity (called $\Sigma\Delta F$) may not be seen as an approximation for the total binding free-energy of the entire peptide—assuming that the residues are independent is certainly a poor approximation—but just as a useful index for analysis. We found that $\Sigma\Delta F$ is −372 kJ/mol for QBP1, −340 kJ/mol for AuBP1, and −376 kJ/mol for AuBP2. On the basis of these values, and considering that the error bar for the adsorption energy of each amino acid is around ±2 kJ/mol, QBP1 should be a gold-binder comparable to AuBP2 and even better than AuBP1. Despite the expectation that there is a high gold-binding capability of QBP1 indicated by these $\Sigma\Delta F$, the conformation of QBP1 prevents the potential gold-binding amino acids to interact effectively with the solid gold surface. In fact, the analysis of atomic contacts between the peptides and the Au surface provides a picture that reveals which parts of the peptides are in direct interaction with the surface. To graphically represent the results of this analysis, we report, in Figure 8, a stick-and-ball representation of the three peptides

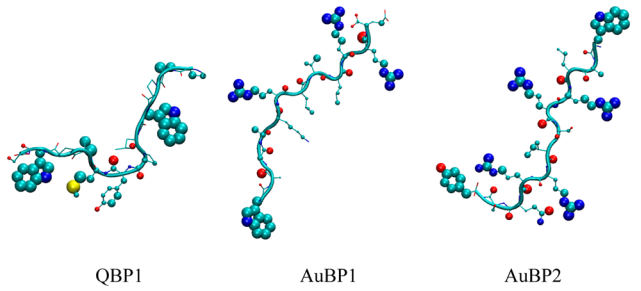

Figure 8. Stick-and-ball representations of the peptides conformation on the surface where the radius of the spheres is proportional to the probability of being in contact with the surface extracted from the REMD simulation.

where the radius of each atom is proportional to the probability of being in contact with the surface as extracted from the REMD simulations. The larger is the atom size, the longer is the time spent in contact with the surface during the simulation.

For AuBP1 and AuBP2, the atoms constantly in contact with the surface, that is, the large atoms in Figure 8, are those belonging the side chain of Trp, Tyr, Arg, that is, the potential Au-binding amino acids that we discussed in the Introduction on the basis of the experimental results[20,52,53] and agreeable with the previous computational studies.[42−44] Notably, the backbone oxygen of the peptide group is also in contact with the surface much more frequently than the amidic nitrogen. Because of geometrical constraints they cannot be both on the surface at the same time. In fact, previous DFT calculations showed that the O tends to stay closer to Au than the N.[44b,54b] The most interesting results of this analysis are for QBP1. In fact, for QBP1 only three of its four potential Au-binding amino

acids (the two Trp and Met) have long-term contacts with the surface, while the small size of Tyr side chain atoms in the figure indicates that Tyr is not frequently touching the surface. Therefore, the potential gold affinity contributed by Tyr residue is not realized in practice, since Tyr seldom contacts gold.

The atom sizes depicted in QBP1 are actually the average values resulting from two distinct arrangements of the peptide on the surface: the prevalent orientations have the two Trp and Met touching the surface and Tyr pointing away from it. Therefore, the minority orientation has Tyr on the surface and one of the other three amino acids away from it. In fact, an analysis of the three-dimensional structure of the adsorbed QBP1, determined by considering the specific order of residues in the sequence, reveals that the four potential gold-binding amino acids point in different spatial directions and do not contact the surface all at the same time. This is different from the AuBPs, where at least four (for AuBP1) and six (for AuBP2) potential Au-binding amino acids simultaneously interact with the gold surface. Also, the backbone of QBP1 is in contact with the gold surface much less frequently than for either of the two AuBPs, which further impairs QBP1 binding. These properties of the peptide are explained by considering the unfavorable molecular folding structures of QBP1 which are imposed by the geometrical constraints dictated by the prolines whose individual and combined effects depend on their specific position in the sequence. Pro's are the origin of the rigidity of QBP1 already noted above. The specific role of peptide flexibility will be discussed in the next section.

3.6. On the Role of Peptide Flexibility. In this section we discuss the flexibility of the three peptides making use of two kinds of analysis: (i) We calculate the end-to-end distance distribution during the last 1.5 ns of the REMD calculations for the three peptides, and (ii) we estimate, *via* an approximate procedure,[82,83] the configurational entropy of the peptides in solution and on the surface, again during the last 1.5 ns of the REMD.

(i) End-to-end distance distributions. This quantity, typically considered for polymeric chains, allows a comparison of the three peptides studied herein with a common reference system: a polymer random chain having typical protein random coil persistence length.[84] Although a 12-mer peptide is too short to statistically behave as a random chain, the latter is still useful since it represents the theoretical upper limit of a "completely flexible" peptide. The normalized distributions of the end-to-end distance for all the three peptides are reported in Figure 9. From these results, a qualitative flexibility order for the peptides can be obtained: AuBP2 is more flexible than AuBP1 which, in turn, is more flexible than QBP1. In fact, the latter has a well-defined peak at a distance around 6 Å, which accounts for most of the probability density integral. This peak corresponds to the conformation Cl.1 in Figure 2. The sharpness of the peak is particularly indicative of the rigidity of the structure.

In contrast, AuBP2 has a very broad and continuous distribution, which is a clear sign of a highly flexible structure. The broad distribution also suggests that, for AuBP2, the subdivision of conformations in clusters is rather artificial, since the peptide structure is changing continuously from compact (small values of the end-to-end distance) to extended. Nevertheless, AuBP2 is still far from the random chain limit.

AuBP1 has an intermediate behavior between QBP1 and AuBP2: it shows a clear peak at around 5 Å (corresponding to Cl.1 in Figure 3), but this peak is much broader than that for QBP1, and a long tail extends to larger end-to-end distances.

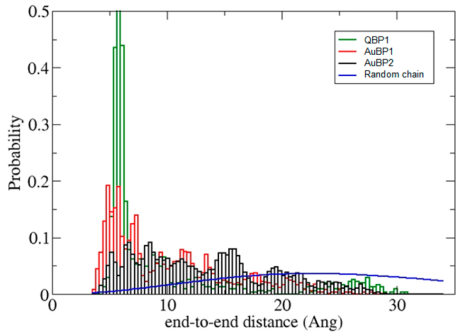

Figure 9. Normalized end-to-end distance distribution for the three peptides AuBP1, AuBP2, and QBP1, in solution (i.e., no gold substrate present) The continuous line refers to the theoretical distribution predicted for a random polymeric chain with typical random coil protein parameters.[84]

(ii) A more quantitative and comprehensive measure of the peptide flexibility is its configurational entropy. It is well-known that to calculate configurational entropy from a MD simulation is a difficult task since it requires, in principle, to sample the entire phase space. Nevertheless, approximate methods have been proposed. Here, we have used the Schlitter's equation[82] which exploits a quasi-harmonic quantum mechanical formulation for the configurational entropy. This method, although approximate, has been tested extensively on peptides.[83] We have omitted rigid translations and rigid body rotations from the entropy, since they are probably not adequately sampled for an entropy calculation, at least for the peptides on Au(111). Overall rotations cannot be exactly decoupled by internal degrees of freedom for flexible peptides; this creates an acceptable uncertainty of around 0.05 to 0.08 kJ/K mol on the heptapeptide entropy calculated in ref 83.

The resulting values for the configurational entropy are reported in Table 4 (S_{conf}), as calculated during the last 1.5 ns of the REMD simulations of the peptides in solution. Since entropy is an extensive quantity, in the same table we also report S_{conf} normalized for the number of atoms in the peptide. Both the total entropy and the normalized quantity provide a picture similar to that found from end-to-end distance distribution (noting that the configurational entropy is also sensitive to side chain conformations), pointing to AuBP2 as the most flexible of the three peptides and QBP1 as the most rigid. AuBP1 is very similar to AuBP2 in terms of S_{conf}. Upon increasing the REMD time interval used from 1.5 to 3 ns, all the S_{conf} increase by only 5−8%, leaving our conclusions unchanged.

In sect. 3.4 we have seen how the configurational flexibility of AuBP1 and AuBP2 favor their interaction with gold, allowing rearrangements of the structure. Flexibility indeed enables these enthalpic gains upon adsorption, but it also implies entropic penalties. In fact, when the peptide is adsorbed on the surface the portion of phase space spanned by its internal degrees of freedom is greatly reduced. The corresponding entropy loss is quantified in Table 4. From these data, it is clear that AuBP2 and AuBP1 pay a higher entropic price upon adsorption than QBP1, whose configuration space is quite limited also in solution. Notably, the ΔS_{conf} reported in the table corresponds to positive contributions to adsorption free energy ($-T\Delta S_{conf}$) ranging from ∼85 kJ/mol to ∼280 kJ/mol, that is, they are of the same order of magnitude as the E^{int} presented in Table 3.

dx.doi.org/10.1021/jp404057h | J. Phys. Chem. C 2013, 117, 16990−17003

Table 4. Configurational Entropy of the Three Peptides Studied in Solutions and Configurational Entropy Variation upon Adsorption

	S_{conf} (kJ/K mol)	S_{conf} (J/K mol)/N atoms	ΔS_{conf} (kJ/K mol)	ΔS_{conf} (J/K mol)/N atoms
AuBP1	5.28	24.3	−0.84	−8.18
AuBP2	5.70	24.7	−0.93	−8.25
QBP1	3.89	19.2	−0.28	−2.64

Therefore, a form of enthalpy−entropy compensation is at work for peptide adsorption.

CONCLUSIONS

In this article, we have presented experimental data showing clearly that peptides selected to bind gold (AuBP1 and AuBP2) have indeed a higher affinity for gold than a peptide selected for quartz, QBP1. By using REMD simulations, we have then provided a microscopic characterization of the structure and flexibility of the three peptides and of their binding to Au(111) surface in water. The main points of our findings are as follows:

- QBP1 presents a relatively well-defined backbone structure in solution due to its high proline contents. On the contrary, AuBP1 and, even more, AuBP2 have floppy structures and adopt different conformations in solution.
- Normally intrinsically disordered AuBP1 and AuB2 conform into dominant folding patterns when in contact with the gold surface. Specifically, upon adsorption on Au(111), atomistic REMD predicts that all the studied peptides change their conformations. The driving force of such changes is the maximization of the direct contacts between the surface and the backbone and the side chains of potential Au-binding amino acids.
- The two gold binding peptides, AuBP1 and AuBP2, have stronger interactions with the gold surface than QBP1 does, as they can reach conformations where more atoms are in contact with the surface. QBP1 has the same number of potential Au-binding amino acids as AuBP1, but not all of them can be in contact with the gold surface at the same time.
- The intrinsic flexibility of the peptide plays an ambiguous role in adsorption onto a solid. A rigid peptide that cannot adopt a conformation in which the potential Au-binding amino acids are able to interact with the gold surface will be a poor gold-binder. Still, nothing prevents this very same peptide to bind effectively to another surface, provided it also contains amino acids suitable to bind to such a surface and properly arranged in space. This is the case of QBP1, that efficiently binds quartz but not gold. On the other hand, a flexible peptide that contains potential Au-binding amino acids (such as AuBP1 and AuBP2) can promptly adapt to the surface, allowing all such amino acids to interact with gold. The peptide−solid interaction is analogous to molecular recognition in biology, where the peptides adapt their conformational folding patterns to the binding cleft of the partner biomolecule. However, the flexibility of the peptide comes with a price: a flexible peptide in solution has higher configurational entropy than a rigid one. Since both rigid and flexible peptides end up in a rather constrained conformation on the surface, the flexible peptide will pay a higher configurational entropy penalty than a rigid one upon adsorption.

On the basis of our findings, we can conclude that AuBP1 and AuBP2 belong to a class of GEPIs characterized by (i) the presence of amino acids with an intrinsic high affinity for the target surface and (ii) a high flexibility that allows them to fully exploit such affinity by maximizing the contact with the surface, paying an acceptable entropic penalty. It is likely that specificity for gold versus other inorganic solid surfaces will be mostly based on the intrinsic preferences of the amino acids as well as the overall peptide structure on the surface, specifically how the prevalent amino acids are brought in contact with the surface versus in the solution.

One can also speculate that another class of gold-binding peptide(s) may exist, and this class would have even higher affinity for gold than those of AuBP1 and AuBP2. An "ideal" gold binding peptide should be rich in amino acids with the known high affinity for gold; its structure in solution should allow all the gold-binding side chains to touch the surface simultaneously, and its molecular structure should also be rigid, so to avoid paying too much of a conformational entropy price upon adsorption. In AuBP1 and AuBP2, this latter requirement is relaxed to permit the maximizing of the contact of the potential Au-binding amino acids with the gold surface, compromising with the resulting loss of entropy upon adsorption. Nevertheless, an imaginary rigid peptide having the same molecular structure of AuBP1 or AuBP2 on gold substrate would have a higher affinity since no price has to be paid, upon adsorption to the surface, in terms of the configurational entropy. The modification of AuBP1 and AuBP2 had indeed been made leading to more rigid structures using cyclic peptides.[12] It was shown that the cyclic peptides had a gold affinity equal or higher than their linear counterparts. In particular, AuBP2, which in its linear version pays the highest entropic cost upon adsorption, increased its binding affinity when made cyclic. We have not yet studied the cyclic peptides computationally, therefore the extent to which cyclization can affect the direct contact of the peptide with the solid surface is not known for now.

At this point, there is a major question whether the 20 natural amino-acid alphabet is versatile enough to produce dodecapeptides that satisfy all of these conditions. Peptides with rigid structures as short as 10 amino acids have indeed been found,[85] suggesting that configurationally rigid designed dodecapeptides might be possible. It may also be feasible to design a shorter peptide that would satisfy all the requirements concurrently for strong solid binding, such as to a gold substrate, using a mixture of natural and non-natural amino acids.

ASSOCIATED CONTENT

Supporting Information

Figure S1, raw SPR kinetic data for the binding of AuBP1, AuBP2, and QBP1 on gold; Figure S2, populations of the conformational clusters from REMD of AuBP1, AuBP2, and QBP1 on Au(111) as a function of REMD time; Figure S3, replica diffusion in temperature space; Figure S4, convergence

dx.doi.org/10.1021/jp404057h | J. Phys. Chem. C 2013, 117, 16990−17003

of the probability orientation of Figure 6 with the REMD time interval. This material is available free of charge via the Internet at http://pubs.acs.org.

AUTHOR INFORMATION

Corresponding Author

*E-mail: stefano.corni@nano.cnr.it; sarikaya@u.washington.edu.

Present Address

[§]University of Kansas, Mechanical Engineering Department, Bioengineering Center, Lawrence, KS 66046, USA.

Notes

The authors declare no competing financial interest.

ACKNOWLEDGMENTS

S.C. thanks the Italian Institute of Technology, Platform "Computation", under the grant project seed "MOPROSURF" for funding and CINECA for the computational time under the INFM "Calcolo parallelo" and ISCRA initiatives. The funding (MH, CT, and MS) was supported by NSF-BMAT (DMR-0706655) and NSF-MRSEC programs (DMR-0520567), *via* GEMSEC, Genetically Engineered Materials Science and Engineering Center, University of Washington, Seattle, WA, USA.

REFERENCES

(1) Addadi, L.; Weiner, S. Control and design principles in biological mineralization. *Angew. Chem., Int. Ed. Engl.* **1992**, *31*, 153−169.

(2) Juliano, D. J.; Saavedra, S. S.; Truskey, G. A. Effect of the conformation and orientation of adsorbed fibronectin on endothelial cell spreading and the strength of adhesion. *J. Biomed. Mater. Res.* **1993**, *27*, 1103−1113.

(3) Yeh, Y.; Feeney, R. E. Antifreeze proteins: Structures and mechanisms of function. *Chem. Rev.* **1996**, *96*, 601−617.

(4) Sarikaya, M. Biomimetics: Materials fabrication through biology. *Proc. Natl. Acad. Sci USA* **1999**, *96*, 14183−14185.

(5) Sarikaya, M.; Tamerler, C.; Jen, A. K.-Y.; Schulten, K.; Baneyx, F. Molecular biomimetics: Nanotechnology through biology. *Nat. Mater.* **2003**, *3*, 577−585.

(6) Gray, J. J. The interaction of proteins with solid surfaces. *Curr. Opin. Struct. Biol.* **2004**, *14*, 110−115.

(7) Brown, S. Engineered iron oxide-adhesion mutants of the *Escherichia coli* phage lambda receptor. *Proc. Natl. Acad. Sci. U.S.A.* **1992**, *89*, 8651−8655.

(8) Perl-Treves, D.; Kessler, N.; Izhaky, D.; Addadi, L. Monoclonal antibody recognition of cholesterol monohydrate crystal faces. *Chem. Biol.* **1996**, *3*, 567−577.

(9) Brown, S.; Sarikaya, M.; Johnson, E. A genetic analysis of crystal growth. *J. Mol. Biol.* **2000**, *299*, 725−735.

(10) Whaley, S. R.; English, D. S.; Hu, E. L.; Barbara, P. F.; Belcher, A. M. Selection of peptides with semiconductor binding specificity for directed nanocrystal assembly. *Nature* **2000**, *405*, 665−668.

(11) Nam, K. T.; Kim, D.-W.; Yoo, P. J.; Chiang, C.-Y.; Meethong, N.; Hammond, P. T.; Chiang, Y.-M.; Belcher, A. M. Virus-enabled synthesis and assembly of nanowires for lithium ion battery electrodes. *Science* **2006**, *312*, 885−888.

(12) Artzy-Schnirman, A.; Zahavi, E.; Yeger, H.; Rosenfeld, R.; Benhar, I.; Reiter, Y.; Sivan, U. Antibody molecules discriminate between crystalline facets of a gallium arsenide semiconductor. *Nano Lett.* **2006**, *6*, 1870−1874.

(13) Kacar, T.; Ray, J.; Gungormus, M.; Oren, E. E.; Tamerler, C.; Sarikaya, M. Quartz binding peptides as molecular linkers towards fabricating multifunctional micropatterned substrates. *Adv. Mater.* **2009**, *21*, 295−299.

(14) Dickerson, M.; Sandhage, K.; Naik, R. R. Protein-and peptide-directed syntheses of inorganic materials. *Chem. Rev.* **2008**, *108*, 4935−4978.

(15) Wei, J. H.; Kacar, T.; Tamerler, C.; Sarikaya, M.; Ginger, D. S. Nanopatterning peptides as bifunctional inks for templated assembly. *Small* **2009**, 689−693.

(16) Nochomovitz, R.; Amit, M.; Matmor, M.; Ashkenasy, N. Bioassisted multi-nanoparticle patterning using single-layer peptide templates. *Nanotechnology* **2010**, *21*, 145305.

(17) Carter, J. D.; LaBean, T. H. Organization of inorganic nanomaterials via programmable DNA self-assembly and peptide molecular recognition. *ACS Nano* **2011**, *5*, 2200−2205.

(18) Hnilova, M.; So, C. R.; Oren, E. E.; Wilson, B. R.; Kacar, T.; Tamerler, C.; Sarikaya, M. Peptide-directed co-assembly of nanoprobes on multimaterial patterned solid surfaces. *Soft Matter* **2012**, *8*, 4327−4334.

(19) Kacar, T.; Zin, M. T.; So, C.; Wilson, B.; Ma, H.; Gul-Karaguler, N.; Jen, A. K.-Y.; Sarikaya, M.; Tamerler, C. Directed self-immobilization of alkaline phosphatase on micro-patterned substrates via genetically fused metal-binding peptide. *Biotechnol. Bioeng.* **2009**, *103*, 696−705.

(20) Hnilova, M.; Oren, E. E.; Seker, U. O. S.; Wilson, B. R.; Collino, S.; Evans, J. S.; Tamerler, C.; Sarikaya, M. Effect of molecular conformations on the adsorption behavior of gold-binding peptides. *Langmuir* **2008**, *24*, 12440−12445.

(21) (a) Hansmann, U. H. E. Parallel tempering algorithm for conformational studies of biological molecules. *Chem. Phys. Lett.* **1997**, *281*, 140−150. (b) Sugita, Y.; Okamoto, Y. Replica-exchange molecular dynamics method for protein folding. *Chem. Phys. Lett.* **1999**, *314*, 141−151.

(22) Latour, R. A. Molecular simulation of protein-surface interactions: Benefits, problems, solutions, and future directions. *Biointerphases* **2008**, *3*, FC2−FC12.

(23) Cohavi, O.; et al. Protein−surface interactions: Challenging experiments and computations. *J. Mol. Rec.* **2009**, *23*, 259−262.

(24) Di Felice, R.; Selloni, A. Adsorption modes of cysteine on Au(111): Thiolate, amino-thiolate, disulfide. *J. Chem. Phys.* **2004**, *120*, 4906−4914.

(25) Nazmutdinov, R. R.; Zhang, J. D.; Zinkicheva, T. T.; Manyurov, I. R.; Ulstrup, J. Adsorption and in situ scanning tunneling microscopy of cysteine on Au (111): Structure, energy, and tunneling contrasts. *Langmuir* **2006**, *22*, 7556−7567.

(26) (a) Ghiringhelli, L. M.; Delle Site, L. Phenylalanine near inorganic surfaces: conformational statistics vs specific chemistry. *J. Am. Chem. Soc.* **2008**, *130*, 2634−2638. (b) Ghiringhelli, L. M.; Hess, B.; van der Vegt, N. F.; Delle Site, L. Competing adsorption between hydrated peptides and water onto metal surfaces: From electronic to conformational properties. *J. Am. Chem. Soc.* **2008**, *130*, 13460−13464.

(27) Hong, G.; Heinz, H.; Naik, R. R.; Farmer, B. L.; Pachter, R. Toward understanding amino acid adsorption at metallic interfaces: A density functional theory study. *ACS Appl. Mater. Interface* **2009**, *1*, 388−392.

(28) Iori, F.; Corni, S.; Di Felice, R. Unraveling the interaction between histidine side chain and the Au(111) surface: A DFT study. *J. Phys. Chem. C* **2008**, *112*, 13540−13545.

(29) Calzolari, A.; Cicero, G.; Cavazzoni, C.; Di Felice, R.; Catellani, A.; Corni, S. Hydroxyl-rich β-sheet adhesion to the gold surface in water by first-principle simulations. *J. Am. Chem. Soc.* **2010**, *132*, 4790−4795.

(30) Braun, R.; Sarikaya, M.; Schulten, K. Genetically engineered gold-binding polypeptides: structure prediction and molecular dynamics. *J. Biomater. Sci.* **2002**, *13*, 747−757.

(31) Bizzarri, A. R.; Costantini, G.; Cannistraro, S. MD simulation of a plastocyanin mutant adsorbed onto a gold surface. *Biophys. Chem.* **2003**, *106*, 111−123.

(32) Setty-Venkat, A.; Corni, S.; Di Felice, R. Electronic coupling between azurin and gold at different protein/substrate orientations. *Small* **2007**, *8*, 1431−1437.

(33) Heinz, H.; Farmer, B. L.; Pandey, R. B.; Slocik, J. M.; Patnaik, S. S.; Pachter, R.; Naik, R. R. Nature of molecular interactions of peptides with gold, palladium, and Pd−Au bimetal surfaces in aqueous solution. *J. Am. Chem. Soc.* **2009**, *131*, 9704−9714.
(34) Coppage, R.; Slocik, J. M.; Briggs, B. D.; Frenkel, A. I.; Heinz, H.; Naik, R. R.; Knecht, M. R. Crystallographic recognition controls peptide binding for bio-based nanomaterials. *J. Am. Chem. Soc.* **2011**, *133*, 12346−12349.
(35) Heinz, H.; Vaia, R. A.; Farmer, B. L.; Naik, R. R. Accurate simulation of surfaces and interfaces of face-centered cubic metals using 12−6 and 9−6 Lennard-Jones potentials. *J. Phys. Chem. C* **2008**, *112*, 17281−17290.
(36) Vila Verde, A.; Acres, J. M.; Maranas, J. K. Investigating the specificity of peptide adsorption on gold using molecular dynamics simulations. *Biomacromolecules* **2009**, *10*, 2118−2128.
(37) Vila Verde, A.; Beltramo, P. J.; Maranas, J. K. Adsorption of homopolypeptides on gold investigated using atomistic molecular dynamics. *Langmuir* **2011**, *27*, 5918−5926.
(38) Yu, J.; Becker, M. L.; Carri, G. A. The influence of amino acid sequence and functionality on the binding process of peptides onto gold surfaces. *Langmuir* **2012**, *28*, 1408−1417.
(39) Brown, S. Metal-recognition by repeating polypeptides. *Nat. Biotechnol.* **1997**, *15*, 269−272.
(40) Tamerler, C.; Duman, M.; Oren, E. E.; Gungormus, M.; Xiong, X.; Kacar, T.; Parviz, B. A.; Sarikaya, M. Materials specificity and directed assembly of a gold-binding peptide. *Small* **2007**, *2*, 1372−1378.
(41) Kulp, J. L.; Sarikaya, M.; Evans, J. S. Molecular characterization of a prokaryotic polypeptide sequence that catalyzes Au crystal formation. *J. Mater. Chem.* **2004**, *14*, 2325−2332.
(42) Pandey, R.; Heinz, H.; Feng, J.; Farmer, B. L.; Slocik, J. M.; Drummy, L. F.; Naik, R. R. Adsorption of peptides (A3, Flg, Pd2, Pd4) on gold and palladium surfaces by a coarse-grained Monte Carlo simulation. *Phys. Chem. Chem. Phys.* **2009**, *11*, 1989−2001.
(43) Feng, J.; Pandey, R. B.; Berry, R. J.; Farmer, B. L.; Naik, R. R.; Heinz, H. Adsorption mechanism of single amino acid and surfactant molecules to Au {111} surfaces in aqueous solution: Design rules for metal-binding molecules. *Soft Matter* **2011**, *7*, 2113−2120.
(44) (a) Hoefling, M.; Iori, F.; Corni, S.; Gottschalk, K. E. Interaction of amino acids with the Au(111) surface: Adsorption free energies from molecular dynamics simulations. *Langmuir* **2010**, *26*, 8347−8351. (b) Hoefling, M.; Iori, F.; Corni, S.; Gottschalk, K. E. The conformations of amino acids on a gold(111) surface. *ChemPhysChem* **2010**, *11*, 1763−1767.
(45) (a) Skelton, A. A.; Liang, T.; Walsh, T. R. Interplay of sequence, conformation, and binding at the peptide−titania interface as mediated by water. *ACS Appl. Mater. Interfaces* **2009**, *1*, 1482−1491. (b) Monti, S.; Walsh, T. R. Free energy calculations of the adsorption of amino acid analogues at the aqueous titania interface. *J. Phys. Chem. C* **2010**, *114*, 22197−22206.
(46) Oren, E. E.; Notman, R.; Kim, I. W.; Evans, J. S.; Walsh, T. R.; Samudrala, R.; Tamerler, C.; Sarikaya, M. Probing the molecular mechanisms of quartz-binding peptides. *Langmuir* **2010**, *26*, 11003−11009.
(47) Makrodimitris, K.; Masica, D. L.; Kim, E. T.; Gray, J. J. Structure prediction of protein−solid surface interactions reveals a molecular recognition motif of statherin for hydroxyapatite. *J. Am. Chem. Soc.* **2007**, *129*, 13713.
(48) Bachmann, M.; Goede, K.; Beck-Sickinger, A. G.; Grundmann, M.; Irbäck, A.; Janke, W. Microscopic mechanism of specific peptide adhesion to semiconductor substrates. *Angew. Chem., Int. Ed.* **2010**, *49*, 9530−9533.
(49) Tomasio, S. M.; Walsh, T. R. Modeling the binding affinity of peptides for graphitic surfaces. Influences of aromatic content and interfacial shape. *J. Phys. Chem. C* **2009**, *113*, 8778−8785.
(50) Tomasio, S. M.; Walsh, T. R. Atomistic modelling of the interaction between peptides and carbon nanotubes. *Mol. Phys.* **2007**, *105*, 221−229.
(51) Willett, R. L.; Baldwin, K. W.; West, K. W.; Pfeiffer, L. N. Differential adhesion of amino acids to inorganic surfaces. *Proc. Natl. Acad. Sci. U.S.A.* **2005**, *102*, 7817−22.
(52) Peelle, B. R.; Krauland, E. M.; Wittrup, K. D.; Belcher, A. M. Design criteria for engineering inorganic material-specific peptides. *Langmuir* **2005**, *21*, 6929−6933.
(53) Cohavi, O.; Reichmann, D.; Abramovich, R.; Tesler, A. B.; Bellapadrona, G.; Kokh, D. B.; Wade, R. C.; Vaskevich, A.; Rubinstein, I.; Schreiber, G. A quantitative, real-time assessment of binding of peptides and proteins to gold surfaces. *Chem.—Eur. J.* **2011**, *17*, 1327−1336.
(54) (a) Iori, F.; Corni, S. Including image charge effects in the molecular dynamics. *J. Comput. Chem.* **2008**, *29*, 1656−1666. (b) Iori, F.; Di Felice, R.; Molinari, E.; Corni, S. GolP: An atomistic force-field to describe the interaction of proteins with Au (111) surfaces in water. *J. Comput. Chem.* **2009**, *30*, 1465−1476.
(55) Oren, E. E.; Tamerler, C.; Sahin, D.; Hnilova, M.; Seker, U. O. S.; Sarikaya, M.; Samudrala, R. A novel knowledge-based approach to design inorganic-binding peptides. *Bioinformatics* **2007**, *23*, 2816−2822.
(56) Matthes, D.; de Groot, B. L. Secondary structure propensities in peptide folding simulations: A systematic comparison of molecular mechanics interaction schemes. *Biophys. J.* **2009**, *97*, 599−608.
(57) Jorgensen, W. L.; Tirado-Rives, J. The OPLS potential functions for proteins, energy minimizations for crystals of cyclic peptides and crambin. *J. Am. Chem. Soc.* **1988**, *110*, 1657−1666.
(58) Zhou, R.; Berne, B. J.; Germain, R. The free energy landscape for beta hairpin folding in explicit water. *Proc. Natl. Acad. Sci. U.S.A.* **2001**, *98*, 14931−14936.
(59) Kokh, D.; Corni, S.; Winn, P.; Hoefling, M.; Gottschalk, K.-E.; Wade, R. C. ProMetCS: An atomistic force field for modeling protein−metal surface interactions in a continuum aqueous solvent. *J. Chem. Theory Comp.* **2010**, *6*, 1753−1768.
(60) Schrader, M. E. Wettability of clean metal surfaces. *J. Colloid Interface Sci.* **1984**, *100*, 372−380.
(61) Wright, L. B.; Rodger, P. M.; Corni, S.; Walsh, T. R. GolP-CHARMM: First-Principles Based Force Fields for the Interaction of Proteins with Au(111) and Au(100). *J. Chem. Theory Comp.* **2013**, *9*, 1616−1630.
(62) Patriksson, A.; van der Spoel, D. A temperature predictor for parallel tempering simulations *Phys. Chem. Chem. Phys.* **2008**, *10*, 2073-2077; see also http://folding.bmc.uu.se/remd/index.php.
(63) TINKER Version 4.2 June 2004 - Software Tools for Molecular Design. Washington University: St. Louis, MO, http://dasher.wustl.edu/tinker/.
(64) Daura, X.; Gademann, K.; Jaun, B.; Seebach, D.; Van Gunsteren, W. F.; Mark, A. E. Peptide folding: When simulation meets experiment. *Angew. Chem., Int. Ed.* **1999**, *38*, 236−240.
(65) Hess, B.; Kutzner, C.; van der Spoel, D.; Lindahl, E. GROMACS 4: Algorithms for highly efficient, load-balanced, and scalable molecular simulation. *J. Chem. Theory Comp.* **2008**, *4*, 435−447.
(66) Wang, F.; Stuart, S. J.; Latour, R. A. Calculation of adsorption free energy for solute-surface interactions using biased replica-exchange molecular dynamics. *BioInterphases* **2008**, *3*, 9−18.
(67) (a) Li, X. F.; O'Brien, C. P.; Collier, G.; Vellore, N. A.; Wang, F.; Latour, R. A.; Bruce, D. A.; Stuart, S. J. An improved replica-exchange sampling method: Temperature intervals with global energy reassignment. *J. Chem. Phys.* **2009**, *127*, 164116−10. (b) Li, X. F.; Latour, R. A.; Stuart, S. J. TIGER2: An improved algorithm for temperature intervals with global exchange of replicas. *J. Chem. Phys.* **2009**, *130*, 174106−9.
(68) Laio, A.; Parrinello, M. Escaping free-energy minima. *Proc. Natl. Acad. Sci. U.S.A.* **2002**, *99*, 12562−12566.
(69) Liu, P.; Kim, B.; Friesner, R. A.; Berne, B. J. Replica exchange with solute tempering: A method for sampling biological systems in explicit water. *Proc. Natl. Acad. Sci. U.S.A.* **2005**, *102*, 13749−13754.
(70) Scheinder, J.; Colombi-Ciacchi, L. Specific material recognition by small peptides mediated by the interfacial solvent structure. *J. Am. Chem. Soc.* **2012**, *134*, 2407−2413.

(71) Mijajlovic, M.; Penna, M. J.; Biggs, M. J. Free Energy of Adsorption for a Peptide at a Liquid/Solid Interface via Non-equilibrium Molecular Dynamics. *Langmuir* **2013**, *29*, 2919−2926.
(72) Varshney, A.; Brooks, F. P.; Wright, W. V. Linearly Scalable Computation of Smooth Molecular Surfaces, *IEEE Comp. Graph. Appl.* **1994**, *14*, 19−25.
(73) Humphrey, W.; Dalke, A.; Schulten, K. VMD—Visual Molecular Dynamics. *J. Mol. Graph.* **1996**, *14.1*, 33−38.
(74) Hnilova, M.; Karaca, B. T.; Park, J.; Jia, C.; Wilson, B. R.; Sarikaya, M.; Tamerler, C. Fabrication of Hierarchical Hybrid Structures Using Bio-enabled Layer-by-Layer Self-Assembly. *Biotechnol. Bioeng.* **2012**, *109*, 1120−1130.
(75) Hnilova, M.; Khatayevic, D.; Carlson, A.; Oren, E. E.; Gresswell, C.; Zheng, S.; Ohuchi, F.; Sarikaya, M.; Tamerler, C. Single-step fabrication of patterned gold film array by an engineered multifunctional peptide. *J. Colloid Interface Sci.* **2012**, *365*, 97−102.
(76) Hnilova, M.; So, C. R.; Oren, E. E.; Wilson, B. R.; Kacar, T.; Tamerler, C.; Sarikaya, M. Peptide-directed co-assembly of nanoprobes on multimaterial patterned solid surfaces. *Soft Matter* **2012**, *8*, 4327−4334.
(77) Tamerler, C.; Oren, E. E.; Duman, M.; Venkatasubramanian, E.; Sarikaya, M. Adsorption kinetics of an engineered gold binding peptide by surface plasmon resonance spectroscopy and a quartz crystal microbalance. *Langmuir* **2006**, *22*, 7712−7718.
(78) Pietropaolo, A.; Muccioli, L.; Berardi, R.; Zannoni, C. A chirality index for identifying protein secondary structures. *Proteins* **2008**, *70*, 667−677.
(79) (a) Wright, P. E.; Dyson, H. J. Linking folding and binding. *Curr. Opin. Struct. Biol.* **2009**, *19*, 31−38. (b) London, N.; Movshovitz-Attias, D.; Schueler-Furman, O. The structural basis of peptide-protein binding strategies. *Structure* **2010**, *18*, 188−199.
(80) Yang, M.; Stipp, S. L. S.; Harding, J. H. Biological control on calcite crystallization by polysaccharides. *Cryst. Growth Des.* **2008**, *8*, 4066−4074.
(81) Heinz, H. Computational Screening of Biomolecular Adsorption and Self-Assembly on Nanoscale Surfaces. *J. Comput. Chem.* **2010**, *31*, 1564−1568.
(82) Schlitter, J. Estimation of absolute and relative entropies of macromolecules using the covariance matrix. *Chem. Phys. Lett.* **1993**, *215*, 617−621.
(83) (a) Schaefer, H.; Mark, A. E.; van Gunsteren, W. F. Absolute entropies from molecular dynamics simulation trajectories. *J. Chem. Phys.* **2000**, *113*, 7809−7817. (b) Schaefer, H.; Daura, X.; Mark, A. E.; van Gunsteren, W. F. Entropy calculations on a reversibly folding peptide: Changes in solute free energy cannot explain folding behavior. *Proteins* **2001**, *43*, 45−56.
(84) Fitzkee, N. C.; Rose, G. D. Reassessing random-coil statistics in unfolded proteins. *Proc. Natl. Acad. Sci. U.S.A.* **2004**, *101*, 12497−12502.
(85) Honda, S.; Yamasaki, K.; Sawada, Y.; Morii, H. 10 residue folded peptide designed by segment statistics. *Structure* **2004**, *12*, 1507−1518.